New Deviation Factor of Power Quality using Tensor Analysis and Wavelet Packet Transform

A.J. Ustariz, E.A.C. Plata and H.E. Tacca

Abstract-- **In this paper, a single discriminating indicator to assess the deterioration of power quality (*Deviation Factor of Power Quality*) is proposed using tensor analysis and wavelet packet transform (WPT). This factor can be used in the presence of stationary and non-stationary power quality disturbances. In addition, practical examples are included to validate the deviation factor of power quality.**

Keywords: **Deviation Factor, Power Quality, Tensor Analysis, Wavelet Packet Transform.**

I. Introduction

THE deterioration of power quality is due to transient disturbances (voltage sags, voltage swells, impulses, among others) and also to steady state disturbances (harmonic distortion, unbalance and flicker) [1]. These quality problems have entailed the need for measuring equipment to monitor the electrical networks, such as electric power quality Analyzers. The first step toward power quality assessment is the definition of power quality indices able to quantify the deviation from an ideal reference situation and quantify the detrimental effects of this deviation [2]-[4].

Existing power quality indices are based on the Fourier transform. This transform can provide accurate results only for stationary waveforms. If waveforms are non-stationary, Fourier transform produces large errors for the measured quantities and therefore fails to accurately quantify the electric power quality [6]. Recently, wavelet analysis techniques using have been proposed in the literature as a new tool for monitoring and analysis of disturbances in power systems [7]-[11].

This paper proposes a global deviation indicator based on tensor analysis of electrical power and on wavelet transform. This indicator is used to measure and evaluate the power quality deterioration in n-phase electrical systems. In addition, practical examples are included to validate the power quality deviation measured by the global indicator.

II. Power Quality Deviation Factor

The measurement and evaluation of nonconformities in a power system in disturbed regime can be quantified through the definition of a new global index of power quality, called instantaneous indicator of power quality deviation, which is evaluated each time using the following expression:

$$IDI_{pq} = \sqrt{\frac{\sum_{i=1}^{n}\sum_{j=1}^{n}\left(\wp_{ij} - {}^{\text{ideal}}\wp_{ij}\right)^2}{\sum_{i=1}^{n}\sum_{j=1}^{n} {}^{\text{ideal}}\wp_{ij}^{\,2}}} \tag{1}$$

where the term $\wp_{ij}$ was defined by the authors in [12] and , [13] as the power instantaneous tensor, thus

$$\wp_{ij} = u_i \otimes i_j = \begin{bmatrix} u_1 \\ u_2 \\ \vdots \\ u_n \end{bmatrix} \otimes \begin{bmatrix} i_1 \\ i_2 \\ \vdots \\ i_n \end{bmatrix} = \begin{bmatrix} u_1 i_1 & u_1 i_2 & \cdots & u_1 i_n \\ u_2 i_1 & u_2 i_2 & \cdots & u_2 i_n \\ \vdots & \vdots & \ddots & \vdots \\ u_n i_1 & u_n i_2 & \cdots & u_n i_n \end{bmatrix} \tag{2}$$

here, u_i e i_j refer to the instantaneous tensors of voltage and current in n-phase systems. Similarly, the term ${}^{\text{ideal}}\wp_{ij}$ is defined as the ideal power tensor. Building an ideal power tensor, involves defining an ideal electrical system as a circuit composed of a sinusoidal and balanced voltage source (ideal reference source) feeding a resistive, balanced and linear load (ideal reference load). Under these ideal conditions the ideal power tensor is defined as:

$${}^{\text{ideal}}\wp_{ij} = u^{+}_{i\_(\text{ideal})} \otimes i^{+}_{j\_(\text{ideal})} \tag{3}$$

where $u^{+}_{i\_(\text{ideal})}$ is the ideal tensor of the direct-sequence voltage, and $i^{+}_{j\_(\text{ideal})}$ is the ideal tensor of the direct-sequence current consumed by the reference load in the ideal power system. Moreover, the root mean square of the IDI_{pq}-*indicator* has been called deviation factor of the power quality (DF_{pq}-*factor*), such that:

$$DF_{pq} = \sqrt{\frac{1}{(t_2 - t_1)}\int_{t_1}^{t_2} \frac{\sum_{i=1}^{n}\sum_{j=1}^{n}\left(\wp_{ij} - {}^{\text{ideal}}\wp_{ij}\right)^2}{\sum_{i=1}^{n}\sum_{j=1}^{n} {}^{\text{ideal}}\wp_{ij}^{\,2}}\,dt} \tag{4}$$

here, the interval defined between t_1 y t_2 match the width of the temporal window of observation. A window of 12 cycles is recommended when the working frequency is 60 Hz [14]. The

This work was supported in part by the Universidad Nacional de Colombia, Manizales Branch.

A.J. Ustariz is with the Department of Electrical, Electronic and Computer Engineering, Universidad Nacional de Colombia, Manizales Branch, Manizales–Colombia (corresponding author: Tel./fax: +57 68 879400x55725, e-mail: ajustarizf@unal.edu.co).

E.A.C. Plata is with the Department of Electrical, Electronic and Computer Engineering, Universidad Nacional de Colombia, Manizales Branch, Manizales–Colombia (e-mail: eacanopl@unal.edu.co).

H.E. Tacca is with the Department of Electronic Engineering, Universidad de Buenos Aires, Buenos Aires – Argentina (e-mail: htacca@fi.uba.ar).

Paper submitted to the International Conference on Power Systems Transients (IPST2011) in Delft, the Netherlands June 14-17, 2011

deviation index defined in (4) varies from zero to infinity. The value zero indicates a null deviation regarding the ideal power system. In other words, the instantaneous tensor is equal to the ideal tensor. The infinite value appears in the power system when the ideal power tensor is equal to zero, which only occurs when there is no active power load consumption. No calculations are going to be done in this particular case, and it has been considered that the tensor formulation does not apply (N/A).

III. IDEAL POWER TENSOR ESTIMATION

Under stationary or non-stationary regime, the ideal power tensor is estimated using the WPT transform. Under these conditions, the ideal power tensor estimation depends directly on the wavelet selected and on the level of the multi resolution achieved. In this case, the ideal power tensor is defined by the expressions given in (5):

$$ {}^{\text{ideal}}\wp_{ij} = u^{+}_{i\_(\ell,1)} \otimes i^{+}_{j\_(\ell,1)}; \qquad i^{+}_{j\_(\ell,1)} = \frac{\mathbf{tr}\left(\frac{1}{t_2-t_1}\int_{t_1}^{t_2}\wp_{ij}\,dt\right)}{\frac{1}{t_2-t_1}\int_{t_1}^{t_2}\left\|u^{+}_{i\_(\ell,1)}\right\|^2 dt}\,u^{+}_{i\_(\ell,1)} \tag{5} $$

here, $u^{+}_{i\_(\ell,1)}$ represents the instantaneous tensor of direct-sequence voltage in the frequency band level ℓ at node 1. It is recommended that the frequency band level ℓ at node 1 is centered at the fundamental frequency. On the other hand, the instantaneous Fortescue transformation [15] is applied to the instantaneous voltage tensor u_i to determine the direct sequence component in an n-phase system. That is,

$$ u_1^{+} = \frac{1}{n}\left(u_1 + a^{-(n-1)}u_2 + \cdots + a^{-2}u_3 + a^{-1}u_n\right) \tag{6} $$

Here, the operator a is defined as $a = e^{j2\pi/n}$. Furthermore, in the time-frequency domain, the waveform of the direct-sequence voltage u^{+}_1 with 2^N samples can be expressed in terms of wavelet coefficients of the WPT transform according to the following equation:

$$ \begin{aligned} u_1^{+} &= \sum_{k=0}^{2^{N-\ell}-1} d^{+}_{1\_(\ell,0,k)}\phi_{(\ell,0,k)} + \sum_{m=1}^{2^{\ell}-1}\left(\sum_{k=0}^{2^{N-\ell}-1} d^{+}_{1\_(\ell,m,k)}\psi_{(\ell,m,k)}\right) \\ &= u^{+}_{1\_(\ell,0)} + \sum_{m=1}^{2^{j}-1} u^{+}_{1\_(\ell,m)} \end{aligned} \tag{7} $$

Now, separating the wavelet coefficients in node 1 at ℓ level, gives:

$$ u_1^{+} = u^{+}_{1\_(\ell,1)} + \left[u^{+}_{1\_(\ell,0)} + \sum_{m=2}^{2^{j}-1} u^{+}_{1\_(\ell,m)}\right] \tag{8} $$

Finally, the inverse Fortescue instantaneous transformation allows the instantaneous tensor of direct sequence voltage in the frequency band level ℓ at node 1, as follows:

$$ u^{+}_{i\_(\ell,1)} = \begin{bmatrix} u^{+}_{1\_(\ell,1)} \\ u^{+}_{2\_(\ell,1)} \\ \vdots \\ u^{+}_{n\_(\ell,1)} \end{bmatrix} = u^{+}_{1\_(\ell,1)} \begin{bmatrix} 1 \\ a^{-1} \\ \vdots \\ a^{-(n-1)} \end{bmatrix} \tag{9} $$

The following is the numerical procedures for these calculations.

IV. POWER QUALITY DETERIORATION ASSESSMENT

This section provides the basis for algorithmic implementation of the proposed global indicator, in its instantaneous (*IDI_{pq}-indicator*) and effective (*DF_{pq}-factor*) versions, when applied to multiphase electrical systems. Two numerical examples have been included in this section to demonstrate the calculation of the power quality deterioration indicator. The first example takes into consideration the stationary waveforms, while the second considers the non-stationary waveforms.

In both examples, the ideal tensor of power, the *IDI_{pq}-indicator* and the *DF_{pq}-factor* are calculated using the proposed method of WPT transform. The result is compared with the true values and the error associated with the method is obtained. Furthermore, db30 is the mother wavelet used in both examples and a temporal observation window of 12 cycles of 60 Hz with a sampling frequency of 10.24 kHz (2048 samples per window) has been selected for the analysis.

A. Numerical example #1: stationary waveforms

In this example, the voltage waveform and the current are distorted by the harmonic components. Values are shown in Table I. The voltage waveforms are stationary, unbalanced and affected by a low frequency signal of direct- sequence of 18 volt amplitude at 20 Hz

TABLE I
STATIONARY WAVEFORM INFORMATION

Phase	VOLTAGE		CURRENT		
	h=1	h=7	h=1	h=5	h=7
1	122∠0º	6.1∠0º	25∠-30º	10∠-150º	5∠-30º
2	127∠-120º	6.4∠-120º	25∠-150º	10∠-30º	5∠-150º
3	110∠120º	5.5∠120º	25∠90º	10∠90º	5∠90º

Step 1 (Calculation of the instantaneous tensors of voltage, current and power): in this example the voltage instantaneous tensor is given by:

$$ u_i = \begin{bmatrix} 18\sin(\omega t/3) + 122\sin(\omega t) + 6.1\sin(7\omega t + 0^{\circ}) \\ 18\sin(\omega t/3 - 120^{\circ}) + 127\sin(\omega t - 120^{\circ}) + 6.4\sin(7\omega t - 120^{\circ}) \\ 18\sin(\omega t/3 + 120^{\circ}) + 110\sin(\omega t + 120^{\circ}) + 5.5\sin(7\omega t + 120^{\circ}) \end{bmatrix} \tag{10} $$

And the current instantaneous tensor by:

$$ i_j = \begin{bmatrix} 25\sin(\omega t - 30^{\circ}) + 10\sin(5\omega t - 150^{\circ}) + 5\sin(7\omega t - 30^{\circ}) \\ 25\sin(\omega t - 150^{\circ}) + 10\sin(5\omega t - 30^{\circ}) + 5\sin(7\omega t - 150^{\circ}) \\ 25\sin(\omega t + 90^{\circ}) + 10\sin(5\omega t + 90^{\circ}) + 5\sin(7\omega t + 90^{\circ}) \end{bmatrix} \tag{11} $$

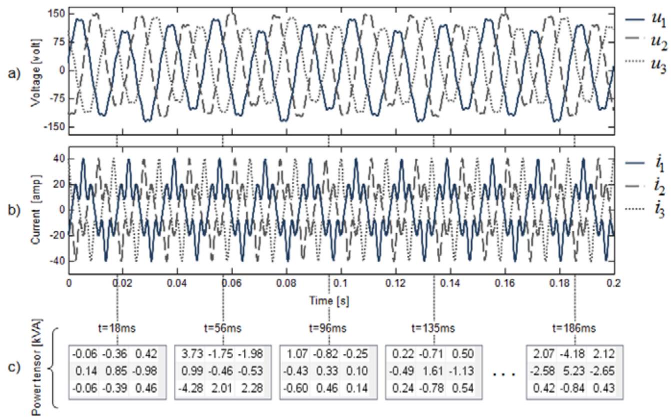

Fig. 1. Stationary numerical results: (a) voltage, (b) current and (c) power instantaneous tensor

Figs. 1(a) and 1(b) show the voltage and current stationary waveforms. The dyadic product between the tensors in (10) and (11) determines the instantaneous power tensor. The mathematical expression of the power tensor is too long thus cannot be shown. However, Figure 1(c) shows several tensors evaluated at *t = 18ms, 56ms, 96ms, 135ms and 186ms*.

Step 2 (Ideal power tensor estimation):

Initially, the true values are determined to compare the relative accuracy of the WPT transform using the already known trigonometric expressions of the waveforms.

Step 2A (True values): applying the Fortescue transform to the voltage waveforms, gives:

$$u_1^+ = 18\sin(\omega t/3) + 119.67\sin(\omega t) + 5.98\sin(7\omega t) \tag{12}$$

Consequently, the true value of the ideal voltage tensor is:

$$u_{i\_(\text{ideal})}^+ = 119.7\begin{bmatrix}\sin(\omega t)\\ \sin(\omega t - 120^\circ)\\ \sin(\omega t + 120^\circ)\end{bmatrix} \tag{13}$$

And therefore, the true value of the ideal current tensor is:

$$i_{j\_(\text{ideal})}^+ = 21.87\begin{bmatrix}\sin(\omega t)\\ \sin(\omega t - 120^\circ)\\ \sin(\omega t + 120^\circ)\end{bmatrix} \tag{14}$$

The dyadic product between the tensors given in (13) and (14) determines the true value of the ideal power tensor

Step 2B (Values based on WPT): In this case the WPT transform (db30, 7 levels) is applied to the direct-sequence component u^+_1, having as a result a multiresolution time-frequency analysis.

The coefficient of multiresolution corresponding to the frequency band (40-80) Hz is the only one used to reconstruct the ideal component $u^+_{1\_(7,1)}$. The ideal voltage, current and power tensors are obtained using these results.

Fig. 2 shows the calculation process used to determine the frequency band component (40-80) Hz of the instantaneous voltage tensor. The waveform of the direct-sequence component, the multiresolution time-frequency analysis and the waveform of the frequency band component (40-80) Hz are shown here.

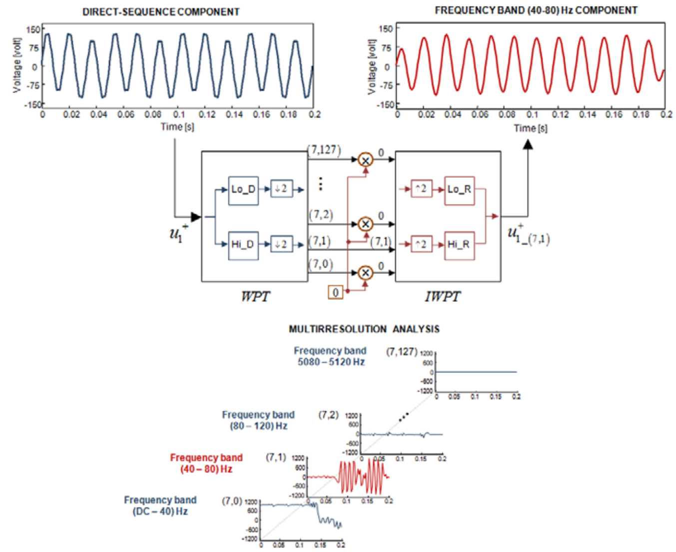

Fig. 2. Stationary numerical results: calculation process of the frequency band component (40-80) Hz

Fig. 2 also shows the suppression process of level 7 multiresolution coefficients, with the exception of the Node 1 component.

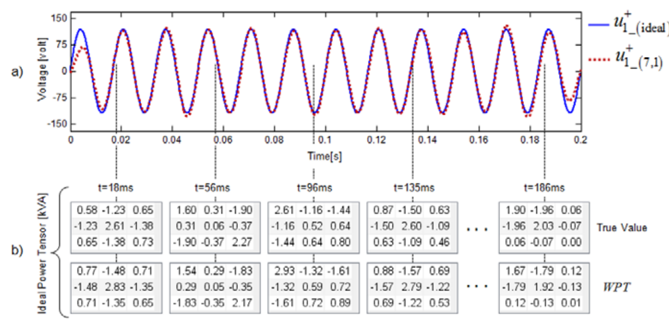

Fig. 3. Stationary numerical results: (a) waveforms of ideal direct-sequence voltage, (b) ideal power tensors

Fig. 3(a) shows the comparison between ideal voltage waveforms ($u^+_{1(\text{ideal})}$ and $u^+_{1(7,1)}$). Fig. 3(b) shows matrices of ideal power tensors (true value and value based on WPT) evaluated at *t = 18ms, 56ms, 96ms, 135ms and 186ms*.

Step 3 (IDI_{pq}-indicator estimation): Fig. 4 shows the comparison between the true value of the power quality instantaneous deviation indicator and the results calculated by the WPT transform.

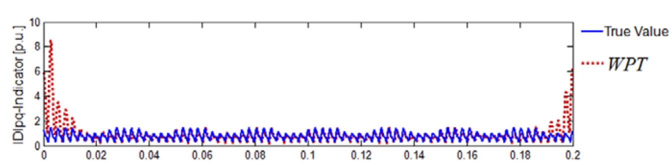

Fig. 4. Stationary numerical results: true value and value based on WPT of the *IDIpq*-indicator.

Fig. 4 also shows that the behavior of the *IDIpq-indicator* calculated by the WPT is acceptable in much of the observation window, except at the borders, where the WPT shows poor indicator estimation.

Step 4 (DFpq-factor estimation): Table II shows the true value, the calculated value, and the errors made when estimating deviation factor of power quality using WPT.

TABLE II
STATIONARY NUMERICAL RESULT (DF_{PQ}-FACTOR)

Factor	True Value	WPT	Relative Error
DF_{pq}	0. 8260 p.u.	1.2185 p.u.	47.52 %

The relative error percentage is calculated using the true value as reference to compare the relative accuracy of the method of WPT transform.

B. *Numerical example #2:non-stationary waveforms*

The voltage waveforms in this example are non-stationary in the temporal observation window. Table III shows the voltage non-stationary waveform information.

TABLE III
VOLTAGE NON-STATIONARY WAVEFORM INFORMATION

Phase	$0.00 \le t < 0.05$	$0.05 \le t < 0.12$	$0.12 \le t < 0.20$	
	h=1	h=1	h=1	h=7
1	120∠0º	35∠60º	100∠0º	15∠0º
2	120∠-120º	58∠-60º	100∠-120º	15∠-120º
3	120∠120º	19∠180º	100∠120º	15∠120º

The calculation procedure for the power quality deterioration global indicator in non-stationary state is the same as the one presented in the example above. Thus, only the results are presented as follows.

Step 1 (Calculation of the instantaneous tensors of voltage, current and power): the voltage instantaneous tensor is given in (15), while the current tensor is same as in (11).

$$u_i = \begin{cases} \begin{bmatrix} 120\sin(\omega t) \\ 120\sin(\omega t - 120^o) \\ 120\sin(\omega t + 120^o) \end{bmatrix} & 0 \le t < 0.05 \\ \begin{bmatrix} 35\sin(\omega t^o) \\ 58\sin(\omega t - 120^o) \\ 19\sin(\omega t + 120^o) \end{bmatrix} & 0.05 \le t < 0.10 \\ \begin{bmatrix} 100\sin(\omega k) + 15\sin(7\omega k + 180^o) \\ 10\sin(\omega k - 120^o) + 15\sin(7\omega k + 60^o) \\ 100\sin(\omega k + 120^o) + 15\sin(7\omega k - 60^o) \end{bmatrix} & 0.10 \le t < 0.20 \end{cases} \quad (15)$$

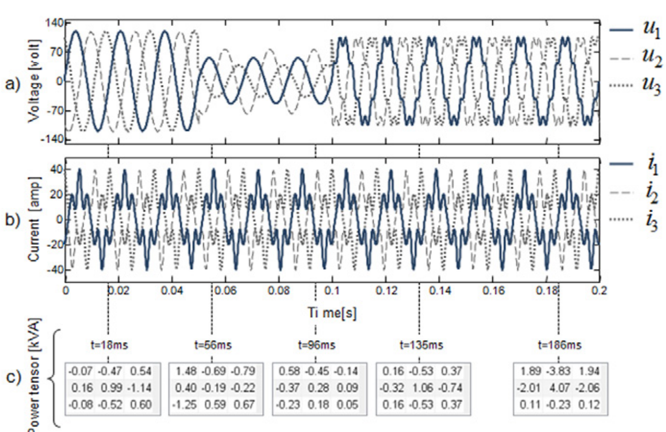

Fig. 5. Non-stationary numerical results: (a) voltage, (b) current and (c) instantaneous power tensor

Figs 5(a) and 5(b) show the voltage and the current non-stationary waveforms. Fig. 5(c) shows several instantaneous power tensors evaluated at *t=18ms, 56ms, 96ms, 135ms y 186ms*.

Step 2 (Ideal power tensor estimation): Fig. 6(a) shows the comparison between the ideal voltage waveforms ($u^+_{1\_(ideal)}$, and $u^+_{1\_(4,1)}$). Fig. 6(b) shows the ideal power tensors matrices (true value and value based on WPT) evaluated at *t=18ms, 56ms, 96ms, 135ms y 186ms*.

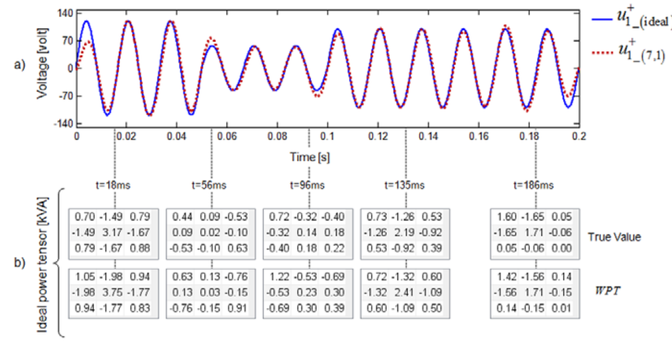

Fig. 6. Non-stationary numerical results: (a) direct-sequence ideal voltage waveforms, (b) ideal power tensors

Step 3 (IDI_{pq}-Indicator estimation): Fig. 7 shows the comparison between the true value of the power quality deviation instantaneous indicator and the results calculated by the WPT transform.

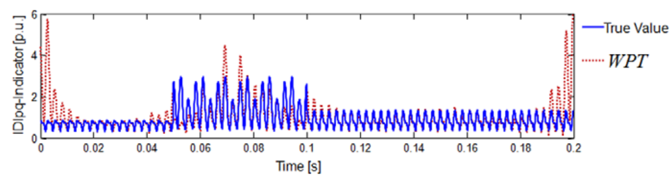

Fig. 7. Non-stationary numerical results: true value and value based on WPT of the *IDIpq*-indicator.

Step 4 (DF_{pq}-Factor estimation): Table IV shows the true value, the calculated value, and the errors made when estimating deviation factor of power quality using WPT. Here, also the relative error percentage is calculated using the true value as reference.

TABLE IV
NON-STATIONARY NUMERICAL RESULTS (DF_{PQ}-FACTOR)

Factor	True Value	WPT	Relative Error
DF_{pq}	1.0714 p.u.	1.2589 p.u.	17.51 %

V. SIMULATED RESULTS

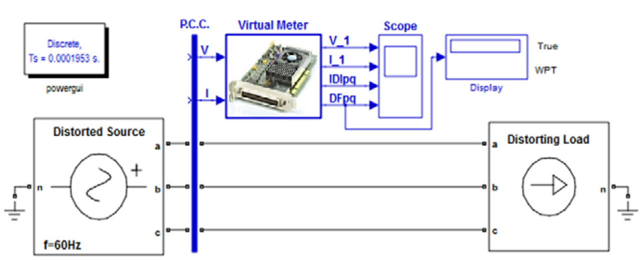

Fig. 8. Scheme of the electrical network and the measurement system

Fig. 8 shows the electrical network and the measurement system implemented in *"Matlab-Simulink"* to realize the validation of the developed calculation procedure in the preceding section.

In order to have the same conditions of comparison between the numerical examples of the previous section and examples simulated in this section, the mother wavelet and temporal observation window used are the same.

A. *Simulated example #1: stationary waveforms*

Fig. 9 shows the simulated results for the stationary case: (a) three-phase voltage waveforms, (b) three-phase current waveforms, (c) IDI_{pq}*-indicator* and (d) DF_{pq}*-factor*.

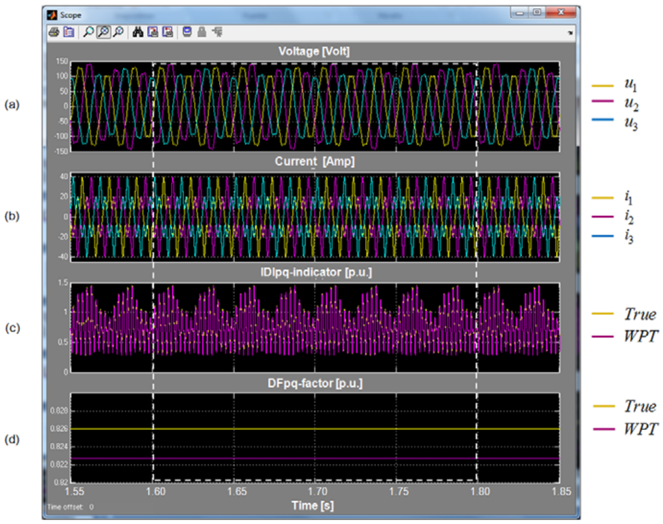

Fig. 9. Simulated results (stationary case)

Table V shows the true values, the simulated values, and the relative error percentage made when estimating deviation factor of power quality using WPT.

TABLE V
STATIONARY SIMULATED RESULTS (DF_{PQ}-FACTOR)

Factor	True Value	WPT	Relative Error
DF_{pq}	0.8260 p.u.	0.8227 p.u.	0.3995%

B. *Simulated example #2: non-stationary waveforms*

Fig. 10 shows the simulated results for the non-stationary case: (a) three-phase voltage waveforms, (b) three-phase current waveforms, (c) IDI_{pq}*-indicator* and (d) DF_{pq}*-factor*.

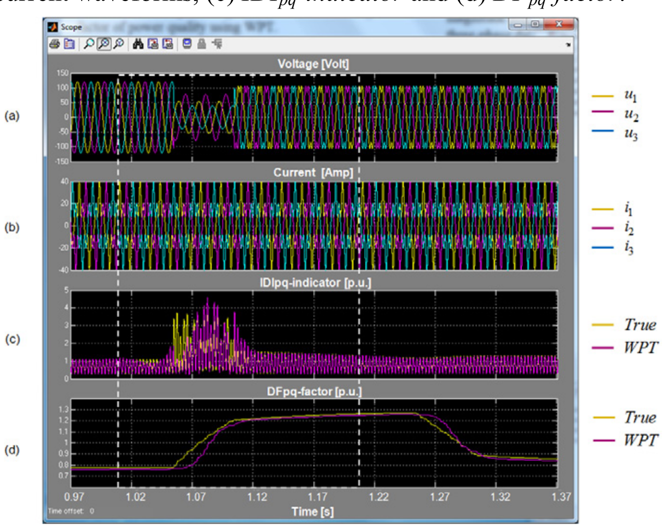

Fig. 10. Simulated results (non-stationary case)

Table VI shows the true values, the simulated values, and the errors made when estimating DF_{pq} power quality deviation factor using WPT (before, during and after of the event).

TABLE VI
NON-STATIONARY SIMULATED RESULTS (DF_{PQ}-FACTOR)

DF_{pq} –Factor (measurement time)	True Value (p.u.)	WPT (p.u.)	Relative Error (%)
before of the event (t=0.97s)	0.7746	0.7610	1.76
during the event (t=1.17s)	1.2478	1.2350	1.03
after of the event (t=1.37s)	0.8542	0.8377	1.93

The Table VI shows that the DF_{pq}*-factor* detects in a global manner any deterioration in the quality of electrical power, independent of the type and origin of the disturbance.

VI. EXPERIMENTAL RESULTS

The algorithm used to estimate the IDI_{pq}*-indicator* and the DF_{pq}*-factor* is summarized in Fig. 11. This algorithm is the core of the measurement virtual instrument designed and built to evaluate the power quality in this research. A dSPACE 1104 control card is used to host the algorithms.

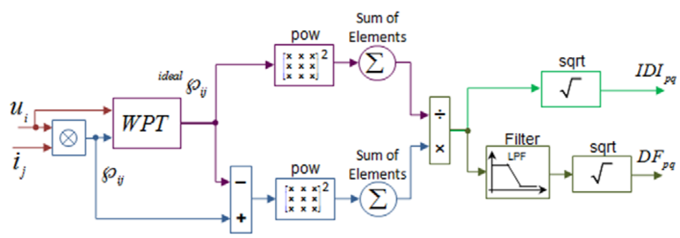

Fig. 11. General algorithmic scheme of the virtual meter

The algorithm was tested with a stationary voltage waveform distorted by harmonic components of low magnitude and imbalanced. The connected non-linear load is a three-phase diode rectifier. The Three-phase of the voltage and current, the IDI_{pq}*-indicator* and DF_{pq}*-factor* were captured with the ControlDesk interface (see Fig.12).

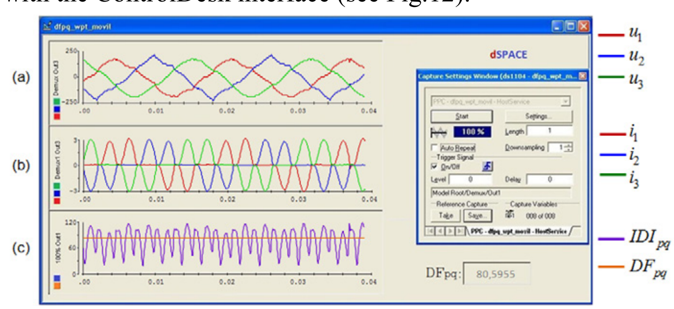

Fig. 12. Experimental results: three-phase diode rectifier

The information in the Fig. 12 is organized as follows: (a) three-phase voltage waveforms, (b) three-phase current waveforms and (c) IDI_{pq}*-indicator* and DF_{pq}*-factor*.

The theoretical, simulation and experimental results show that to use the tensor analysis and wavelet transform is a good method to measure the power quality deterioration in the presence of stationary and non-stationary waveform. Beside, the implementation in a continuous medium (calculation time $\gg$ 12 cycles) allows to diminish the errors in the borders of the temporary window of observation.

VII. Conclusions

An integral evaluation of the power quality deterioration in multiphase networks through a new indicator (in its instantaneous-IDI_{pq} or effective-DF_{pq} versions) has been suggested. The proposed algorithms are based on instantaneous power tensor analysis and on the wavelet packet transform. A method for assessing power quality deterioration has been presented and analyzed taking into account stationary and non-stationary waveforms. The theoretical, simulation and experimental results validate the applicability of the proposed indicator when measuring quality loss.

VIII. Acknowledgment

The authors gratefully acknowledge the work of Y.A. Garcés for their collaboration on the experimental implementation of this document.

IX. References

[1] M.H.J. Bollen, and I.Y.H. Gu, *Signal Processing of Power Quality Disturbances*, John Wiley & Sons, 2006.

[2] P. Salmerón, R.S. Herrera, A. Pérez and J. Prieto, "*New Distortion and Unbalance Indices Based on Power Quality Analyzer Measurements*," IEEE Trans. Power Del., vol. 24, no. 2, pp.501 – 507, Apr. 2009.

[3] A. Ferrero, "*Measuring Electric Power Quality: Problems and Perspectives*," Measurement, vol. 41, no 2, pp.121-129, Feb. 2008.

[4] Y.J. Shin, E.J. Powers, M. Grady, and A. Arapostathis, "*Power Quality Indices for Transient Disturbances*," IEEE Trans. Power Del., vol. 21, no. 1, pp. 253-261, Jan. 2006.

[5] D. Castaldo, A. Ferrero, S. Salicone, and A.Testa, "A power-quality index based on multi-point measurements," *in: Proc. 2003 IEEE Power Tech*, pp. 23–26.

[6] J. Driesen, T. Van Craenenbrock, R. Reekmans, D. Van Dommelen, "Analyzing time-varying power system harmonics using wavelet transform," in: Proc. 1996 Instrumentation and Measurement Technology Conference. IMTC-96, pp. 474–479.

[7] S. Sansoto, M. W. Grady, E. J. Powers, J. Lamoree, S. Bhatt, "*Characterization of Distribution Power Quality Events with Fourier and Wavelet Transforms*," IEEE Trans. on Power Delivery, vol. 15, no. 1, pp. 247-254, Jan. 2000 .

[8] Y. Gu, M. H. J. Bollen, "*Time-Frequency and Time-Scale Domain Analysis of Voltage Disturbances*," IEEE Trans. on Power Delivery, vol. 15, no. 4, pp. 1279-1284, Oct. 2000.

[9] A.M. Gaouda, S.H. Kanoun, M.M.A. Salama, and A.Y. Chikhani, "Wavelet-based signal processing for disturbance classification and measurement," *in IEE Proceedings- Generation, Transmission and Distribution,* vol. 149, no. 3, pp. 310-318, 2002.

[10] M. Wang, G. I. Rowe, and A. V. Mamishev, "*Classification of power quality events using optimal time-frequency representations – Part 2: Application*," IEEE Trans. on Power Delivery, vol. 19, no. 3, pp. 1496-1503, Jul. 2004.

[11] M.A.S. Masoum, S. Jamali, and N. Ghaffarzadeh, "*Detection and classification of power quality disturbances using discrete wavelet transform and wavelet networks*," IET Science Measurement & Technology, vol. 4, no.4,pp. 193 – 205, 2010.

[12] A.J. Ustariz, E.A. Cano and H.E. Tacca, "Tensor analysis of the instantaneous power in electrical networks," *Electric Power Systems Research*, vol. 80, no 7 pp. 788–798, Jul. 2010.

[13] A.J. Ustariz, E.A. Cano, and H.E. Tacca, "Instantaneous Power Tensor Theory: Improvement and Assessment of the Electric Power Quality", *14th International Conference on Harmonics and Quality of Power, ICHQP'2010*, Bergamo-Italy, pp. 1-6, September 2010.

[14] *IEC, Power Quality Measurements Methods, Testing and Measurement Techniques*, IEC Std. 61000-4-30.

[15] C.L Fortescue, "*Method of symmetrical co-ordinates applied to the solution of polyphase networks*," AIEE Transactions, vol. 2, pp. 1027-1140, Jul.1918.

X. Biographies

Armando J. Ustariz Farfan: was born in Urumita (Colombia) in 1973. He received a bachelor's degree in Electrical Engineer in 1997, and a Master's in Electric Power in 2000 from the Universidad Industrial de Santander. He is currently pursuing the Ph.D. degree in Electrical Engineering at the Universidad Nacional de Colombia. Since 2003, he has been with the Faculty of Engineering, Universidad Nacional de Colombia, Manizales Branch, where he is currently with the Electrical, Electronic and Computer Engineering Department. His research interests include power definitions under non-sinusoidal conditions, power quality analysis, and power electronic analysis.

Eduardo A. Cano Plata: was born in Neiva, Colombia, in 1967. He received the B.Sc. and Specialist Engineering degree in 1990 and 1994 from Universidad Nacional de Colombia, Manizales, both in Electrical Engineering. Between 1996 and 1998 he had a DAAD scholarship for postgraduate studies in Electrical Engineering at the Universidad Nacional de San Juan, Argentina. He received the Doctor degree in Engineering in 2006 from the Universidad de Buenos Aires. Since 1994, he is an associated professor at the Universidad Nacional de Colombia in Manizales.

Hernán E. Tacca: was born in Argentina in 1954. He received the B.E. degree in Electrical Engineering from Universidad de Buenos Aires, Argentina in 1981, the M.S. in 1988 and the Ph.D. degree from the University of Sciences and Technologies of Lille, France, in 1993. In 1998 he received the doctorate from Universidad de Buenos Aires. Since 1984, he has been with the Faculty of Engineering, Universidad de Buenos Aires, where he is currently with the Dept. of Electronics, engaged in teaching and research in the areas of Industrial Electronics, leading a laboratory devoted to power electronics (LABCATYP). His research interests are in the fields of SMPS, UPS, battery chargers, soft-switching techniques, and low-cost micro-controller control of power converters.